J Biol Inorg Chem (2001) 6:151–158
DOI 10.1007/s007750000185

ORIGINAL ARTICLE

**Peter P. Schmidt · Reinhard Lange
Antonius C.F. Gorren · Ernst R. Werner
Bernd Mayer · K. Kristoffer Andersson**

Formation of a protonated trihydrobiopterin radical cation in the first reaction cycle of neuronal and endothelial nitric oxide synthase detected by electron paramagnetic resonance spectroscopy

Received: 23 May 2000 / Accepted: 6 October 2000 / Published online: 21 December 2000

Abstract Nitric oxide synthase (EC 1.14.13.39; NOS) converts L-arginine into NO and L-citrulline in a two-step reaction with N^{ω}-hydroxy-L-arginine (NOHLA) as an intermediate. The active site iron in NOS has thiolate axial heme-iron ligation as found in the related monooxygenase cytochrome P450. In NOS, tetrahydrobiopterin (BH_4) is an essential cofactor for both steps, but its function is controversial. Previous optical studies of the reaction between reduced NOS with O_2 at –30 °C suggested that BH_4 may serve as an one-electron donor in the first cycle, implying formation of a trihydrobiopterin radical. We investigated the same reaction under identical conditions with electron paramagnetic resonance spectroscopy. With BH_4-containing full-length neuronal NOS we obtained an organic free radical (*g*-value 2.0042) in the presence of Arg, and a similar radical was observed with the endothelial NOS oxygenase domain in the presence of Arg and BH_4. Without substrate the radical yield was greatly (10×) diminished. Without BH_4, or with NOHLA instead of Arg, no radical was observed. With 6-methyltetrahydropterin or 5-methyl-BH_4 instead of BH_4, radicals with somewhat different spectra were formed. On the basis of simulations we assign the signals to trihydropterin radical cations protonated at N5. This is the first study that demonstrates the formation of a protonated trihydrobiopterin radical with the constitutive isoforms of NOS, and the first time the radical was obtained without exogenous BH_4. These results offer strong support for redox cycling of BH_4 in the first reaction cycle of NOS catalysis ($BH_4 \leftrightarrow BH_3{\bullet}H^+$).

Keywords Nitric oxide synthase · Biopterin · Heme · Oxygen activation · Radical

Abbreviations *Arg*: L-arginine · *BH_4 and tetrahydrobiopterin*: (6*R*)-5,6,7,8-tetrahydro-6-(L-erythro-1′,2′-dihydroxypropyl)pterin · *cyt P450*: cytochrome P450 · *eNOS*: endothelial nitric oxide synthase · *hfc*: hyperfine coupling · *iNOS*: inducible nitric oxide synthase · *5-methyl-BH_4*: (6*R*)-5-methyl-6,7,8-trihydro-6-(L-erythro-1′,2′-dihydroxypropyl)pterin · *6-methyl-PH_4*: 6-methyl-5,6,7,8-tetrahydropterin · *nNOS*: neuronal nitric oxide synthase · *NOHLA*: N^{ω}-hydroxy-L-arginine · *NOS*: nitric oxide synthase

P.P. Schmidt · K.K. Andersson (✉)
Department of Biochemistry, University of Oslo,
PO Box 1041 Blindern, 0316 Oslo, Norway
E-mail: k.k.andersson@biokjemi.uio.no
Phone: +47-2-2856625
Fax: +47-2-2854443

R. Lange
INSERM U128, IFR24, 1919 Route de Mende,
34293 Montpellier Cedex 5, France

A.C.F. Gorren · B. Mayer
Institut für Pharmakologie und Toxikologie,
Karl-Franzens-Universität Graz, Universitätsplatz 2,
8010 Graz, Austria

E.R. Werner
Institut für Medizinische Chemie und Biochemie,
Universität Innsbruck, 6020 Innsbruck, Austria

Introduction

Nitric oxide synthase (EC 1.14.13.39; NOS) catalyzes the formation of the biologically very important reactive nitric oxide (NO) and L-citrulline from L-arginine (Arg) and molecular oxygen, utilizing NADPH-derived electrons for reductive O_2 activation (for recent reviews of NOS, see [1, 2, 3, 4]). All three known NOS isoforms [neuronal (nNOS), endothelial (eNOS), and inducible NOS (iNOS)] are homodimers, with each monomer consisting of a reductase and an oxygenase domain. The FAD- and FMN-containing reductase domain transfers electrons in a calmodulin-dependent manner from NADPH to a cytochrome P450 (cyt P450)-type heme (i.e., thiolate axial heme-

iron ligation) in the oxygenase domain. NO synthesis takes place at the heme in two discrete cycles with $N^{(\omega)}$-hydroxy-L-arginine (NOHLA) being formed as an intermediate. The first monooxygenase cycle requires two electrons, whereas only one electron is necessary in the second cycle [1, 2, 3, 4, 5, 6, 7]. The reductase domain can be replaced by other electron sources for single turnover reactions. The first cycle is thought to involve similar catalytic complexes as proposed for cyt P450 and some peroxidases: (1) substrate binding, forming high-spin ferric NOS, (2) first electron reduction to high-spin ferrous NOS, (3) oxygen binding, forming a superoxide complex (oxy-ferrous) NOS, (4) second electron reduction, forming a peroxide complex, followed by (5) heterolytic cleavage of the O-O bond, forming a compound I type complex (probably with a ferryl iron and π-centered porphyrin radical as one resonance stabilized form), and (6) formation of NOHLA and high-spin ferric NOS, possibly by a radical recombination pathway [3, 4, 5, 6, 7, 8, 9, 10, 11, 12, 13, 14, 15, 16].

NOS is unique among P450-type enzymes in requiring tetrahydrobiopterin [(6*R*)-5,6,7,8-tetrahydro-6-(L-erythro-1′,2′-dihydroxypropyl)pterin; BH_4] as an essential cofactor for NO synthesis, but its mode of action is poorly understood [3, 4, 5, 17, 18]. In the catalytic mechanism of the aromatic amino acid hydroxylases BH_4 undergoes redox cycling with intermediate formation of 4a-hydroxytetrahydrobiopterin and quinonoid dihydrobiopterin (q-BH_2) [19]. However, redox cycling between BH_4 and qBH_2 can be ruled out for NOS catalysis [6, 20]. On the other hand, the effects of BH_4 on NOS that have been documented thus far (dimer stabilization [21, 22], heme low- to high-spin shift [23, 24], and increase of substrate affinity [25, 26]) do not sufficiently explain its essential function as the same effects are produced by pterin-site NOS inhibitors like dihydrobiopterin or 4-amino-BH_4 [27]. In a previous paper we presented an optical study under single turnover conditions at –30 °C, when no transfer of the essential second electron to the superoxide complex from flavins or dithionite can occur, of the reaction between ferrous nNOS and O_2 in the presence and absence of Arg and BH_4 [28]. On the basis of these results we proposed a hitherto unanticipated role for BH_4 as a one-electron donor during NOS catalysis in the first cycle, implying the transient formation of a pterin radical. Indeed, a BH_4-derived radical was recently observed by Marletta and coworkers [29] with the iNOS oxygenase domain.

In the present study we use low-temperature electron paramagnetic resonance (EPR) spectroscopy and the same –30 °C experimental protocol as applied in our previous study [28], to demonstrate the formation of a pterin radical with full-length nNOS in the absence of exogenous BH_4. This is the first report on the generation of a pterin radical by a full-length NOS. This rules out that pterin radical formation is an artefact of the oxygenase domain. We demonstrate pterin radical formation by the two constitutive NOS isoforms which have not been studied by the Marletta group [29]. Furthermore we report quite similar radicals with the eNOS oxygenase domain in the presence of Arg and BH_4, 5-methyl-BH_4, or 6-methyltetrahydropterin (6-methyl-PH_4), which shows that pterin radical formation is common to all isoforms. From spectral simulations we deduce that the BH_4-derived EPR signal can be ascribed to a trihydrobiopterin cation protonated at N5 (BH_3•H^+). The results reported in this study provide strong support for the postulated novel role of BH_4 as a one-electron donor, which also might have implications for the aromatic amino acid hydroxylases.

Materials and methods

Materials

Bovine endothelial NOS oxygenase domain (aa 55–491) was cloned as an *Eco*RI-*Xho*I insert in pGEX4T1 and expressed in *Escherichia coli* as a glutathione-*S*-transferase fusion protein using standard procedures (to be published elsewhere). Recombinant rat brain full-length neuronal NOS was purified from baculovirus-infected insect cells [30]. BH_4 was from Alexis Biochemicals (Laufen, Switzerland); NOHLA was from Sigma (St. Louis, USA); (6*R*)-5-methyl-6,7,8-trihydro-6-(L-erythro-1′,2′-dihydroxypropyl)pterin (5-methyl-BH_4) and 6-methyl-5,6,7,8-tetrahydropterin (6-methyl-PH_4) were from Schirck's Laboratory (Jona, Switzerland).

Methods

Samples were prepared essentially according to Bec et al. [28], except that EPR tubes replaced optical cuvettes. Samples in 50% ethylene glycol, 50 mM sodium phosphate (pH 7.5), were made anaerobic in the EPR tubes by gassing with argon for 1 h at 0 °C. Then the ferric heme was reduced with anaerobic dithionite, final concentration 400 µM, at room temperature. Samples were then cooled to –30 °C, bubbled for 5 s with oxygen, and flash-frozen in –130 °C *n*-pentane after about 30 s reaction time. EPR spectra were recorded at 9.65 GHz on a Bruker ESP300E EPR spectrometer equipped with an Oxford Instruments cryostat 900 (0.5 or 4 mW microwave power, 3 G modulation amplitude, 100 kHz modulation frequency, and temperatures of 4, 9, and 30 K). $P_{1/2}$ values of the microwave power saturation were determined over a microwave power range of 0.3 µW to 200 mW and least-square fitting.

EPR simulations

Least-square fits between simulated and experimental spectra (recorded at 9 K) were obtained with the xemr program from Jussi Eloranta [31], employing the Monte-Carlo method and first-order perturbation theory. The small isotropic hyperfine coupling (hfc) constants found at room temperature for pterin radicals [32, 33, 34, 35] show clearly that N5 and N8 are sp^2 hybridized. Thus, all hfc tensors were assumed to be colinear, i.e. all non-diagonal elements are zero, and are given as row vectors in the text throughout. All hfc constants are given in G.

As the N5 and N8 α- and C6 and C7 β-protons in a protonated trihydropterin radical show similar isotropic coupling constants compared with the nitrogen [32, 33, 34, 35], none of these protons can be neglected and the full simulation must include seven nuclei (see Discussion of Fig. 2 below). Thus, EPR theory

Table 1

Sample	Tensor element	A_I ^{14}N5	A_I N5-H_α	A_I N5-$CH_{3\beta1}$	A_I N5-$CH_{3\beta2}$	A_I N5-$CH_{3\beta2}$	A_I C6-H_β	A_I ^{14}N8	A_I N8-H_α	A_I C7-$H_{\beta1}$	A_I C7-$H_{\beta2}$
Full-length NOS	x	1.5	–3.65	–	–	–	8.79	0.254	–0.905	4.29	1.75
	y	1.0	–18.64	–	–	–	14.27	0.169	–2.944	3.51	1.17
	z	29.8	–16.04	–	–	–	20.31	5.566	–1.550	4.40	2.62
	iso	10.8	–12.8	–	–	–	14.46	2.00	–1.80	4.07	1.85
	ρ	0.43	–	–	–	–	(0.43)	0.080		(0.080)	(0.080)
	θ	–	–	–	–	–	38°	–	–	14°	130°
NOS oxygenase	x	4.6	–5.6	–	–	–	14.4	0.2	–0.6	4.3	1.8
	y	3.4	–22.6	–	–	–	12.9	0.1	–3.2	4.3	1.6
	z	25.2	–12.8	–	–	–	16.0	6.0	–2.2	4.6	2.6
	iso	11.1	–13.7	–	–	–	14.4	2.1	–2.0	4.4	2.0
	ρ	0.44		–	–	–	(0.44)	0.084	–	(0.084)	(0.084)
	q	–	–	–	–	–	39°	–	–	10°	131°
6-CH_3-PH_4	x	4.85	–5.03	–	–	–	14.5	0.54	–1.00	5.70	2.43
	y	5.04	–21.88	–	–	–	13.4	0.66	–4.71	5.61	2.44
	z	25.03	–11.89	–	–	–	16.2	7.13	–3.26	6.16	2.78
	iso	11.6	–12.9	–	–	–	14.7	2.78	–2.99	5.82	2.55
	ρ	0.47	–	–	–	–	(0.47)	0.11	–	(0.11)	(0.11)
	θ	–	–	–	–	–	41°	–	–	8°	130°
5-CH_3-BH_4	x	4.06	–	19.0	13.5	1.02	13.9	0.530	–1.80	5.80	2.64
	y	4.01	–	18.4	13.5	0.90	12.9	0.218	–4.84	5.67	2.53
	z	27.23	–	22.1	15.2	0.78	15.8	9.795	–3.22	7.00	3.30
	iso	11.8	–	19.8	14.1	0.90	14.2	3.51	–3.29	6.16	2.82
	ρ	0.47	–	–	–	–	(0.47)	0.14	–	(0.14)	(0.14)
	θ	–	–	28°	137°	275°	42°	–	–	26°	127°

and geometric considerations were taken into account to restrict the parameter search. The spin density ρ on N5 was kept between 0.4 and 0.5, that on N8 around 0.1 [33, 34]. The Q-factors in the McConnell relation $A_i=Q\rho$ were taken to be 25 G for the nitrogen nucleus [36] and –27 G for an α-proton [33, 36]. The difference in dihedral angles θ, calculated from the Heller-McConnell relation $A_i=(B_0+B_2\cos\theta)\rho$, for the two C7-$H_\beta$ and the three N5-methyl protons in 5-methyl-BH_4 was restricted to 120± 20°. B_0 and B_2 are empirical constants with $B_0<<B_2$; from recent density functional calculations they were found to be 1.5 and 52.4 G, respectively [37]. The isotropic hfc constant of 13 G found for C6-H_β at room temperature [34] then yields $\theta\approx40°$ and suggests 15° and 135° for C7-$H_{\beta1,2}$ by geometric considerations. Nitrogen tensors were kept strongly axial, e.g. (5, 3, 25), α-proton tensors highly rhombic, e.g. (–6, –23, –13), and β-proton tensors isotropic, e.g. (14, 13, 16). The g-tensor was assumed to be isotropic. Errors of ±5% for the hfc constants listed in Table 1 were estimated from the varying results achieved with different start values.

Results

Formation of an organic free radical in full-length BH_4-containing nNOS in the presence of Arg

In a previous low-temperature optical spectroscopic study [28] of the reaction of ferrous NOS with O_2, we found formation of an oxy-ferrous heme (ferric superoxide) intermediate in the absence of Arg or BH_4, whereas the reaction proceeded beyond that species when Arg and BH_4 were both present. We postulated that BH_4 donated the electron required for reductive activation of the oxy-ferrous complex, implying the intermediate formation of a trihydrobiopterin radical

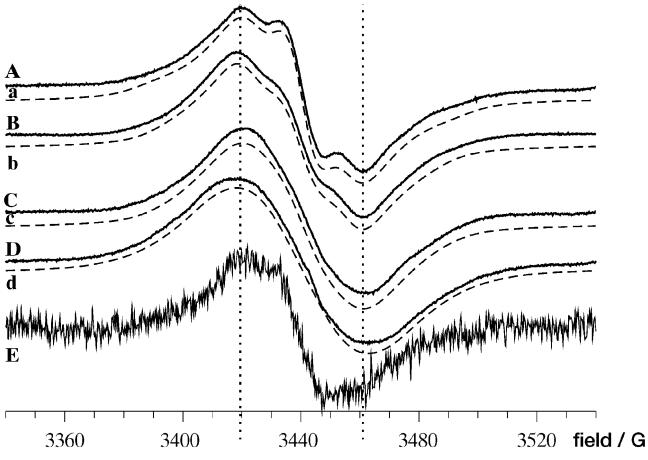

Fig. 1 EPR spectra and simulations of NOS samples after 30 s reaction time at –30 °C. Spectra are base-line corrected and normalized for better comparison. *A* 4 μM full-length nNOS containing endogenous BH_4+500 μM Arg, 0.84 μM radical, 90 scans with a 168 s sweep time. *B* 60 μM eNOS oxygenase+100 μM BH_4+200 μM Arg, 14 μM radical, 1 scan with a 84 s sweep time. *C* 60 μM eNOS oxygenase+70 μM 6-methyl-PH_4+200 μM Arg, 1.7 μM radical, 30 scans with a 168 s sweep time. *D* 33 μM eNOS oxygenase+1 mM 5-methyl-BH_4+500 μM Arg, 1.2 μM radical, 40 scans with a 168 s sweep time. *E* 25 μM eNOS oxygenase+25 μM BH_4, no Arg, 0.64 μM radical, 1 scan with a 84 s sweep time. *a–d* Simulations using the parameters in Table 1. EPR parameters were 9 K, 100 kHz modulation frequency, and 3 G modulation amplitude. Microwave power was 0.5 mW for *A*, *B*, and *C*; 1 mW for *D*; and 4 mW for *E*

[28]. To corroborate our hypothesis we attempted to detect the radical intermediate by EPR spectroscopy. We chose the shortest possible mixing time at –30 °C of 30 s after oxygenation as incubation time.

A 30 s reaction at –30 °C between ferrous full-length BH_4-containing (about 0.5 equivalents BH_4 per dimer) nNOS and O_2 resulted in a free radical signal at g=2.0042±0.0003 (Fig. 1A). The sample shown contained 4 μM nNOS+500 μM Arg in 50% ethylene glycol, 50 mM phosphate buffer. The radical amount was quantified to 0.84 μM by comparison with a $CuClO_4$ standard, i.e. 42% of available BH_4. The radical is readily detected at 4 and 9 K. Its shape and position, and the clearly visible hyperfine interaction, strongly indicate an organic free radical. The corresponding simulated spectrum is shown in Fig. 1a. Satisfactory simulation required spin density on N5 and N8, and protonation of both nitrogens (see Discussion). The resulting hfc tensors for the spin densities on N5 (hfc with one α-proton and one β-proton) and N8 (hfc with one α-proton and two β-protons) are summarized in Table 1. In the second reaction cycle of NOS, i.e. when Arg was replaced by NOHLA in full-length nNOS, no radical was detected under otherwise identical conditions (data not shown).

Formation of a similar free radical by the eNOS oxygenase domain in the presence of Arg and BH_4

Figure 1B shows a typical result with 30 s reaction time at –30 °C of a similar experiment carried out with the eNOS oxygenase domain in the presence of Arg and BH_4. The radical yield was 14 μM, corresponding to 0.23 equiv per heme. The EPR signal is very similar to the one detected in full-length nNOS and is visible in the temperature range from 4 to 30 K. Its simulation with the hfc constants listed in Table 1 is shown in Fig. 1b.

No radical was detected without exogenous BH_4 (data not shown). A control sample without Arg (Fig. 1E), containing 25 μM eNOS oxygenase domain+25 μM BH_4, showed a 10-fold lower radical content (0.026 radical equivalents per NOS heme). As with full-length nNOS, no radical was detected with NOHLA instead of Arg under otherwise identical conditions (data not shown).

Detection of a 6-methyl-PH_4 derived radical in the eNOS oxygenase domain in the presence of Arg

Pterin analogs were studied to corroborate that the radical is situated on the pterin moiety. Figure 1C shows the spectrum obtained with a sample containing 60 μM eNOS oxygenase domain, 70 μM 6-methyl-PH_4, and 200 μM Arg after 40 s reaction time at –30 °C, corresponding to 1.7 μM radical. In comparison with the spectra in Fig. 1A and B the positions of the absolute peak and trough (indicated by the two dotted vertical lines) are not changed but the hyperfine splitting is no longer resolved. The best simulation is displayed in Fig. 1c; for the hfc tensors, see Table 1.

Detection of a 5-methyl-BH_4 derived radical in the eNOS oxygenase domain in the presence of Arg

Figure 1D shows 1.2 μM radical formed in a sample containing 33 μM eNOS oxygenase domain, 1 mM 5-methyl-BH_4, and 500 μM Arg under otherwise analogous conditions. In the presence of 70 μM 5-methyl-BH_4 we could not detect any radical (data not shown). Clearly the peak and trough positions of the radical are shifted to lower and higher field, respectively, compared to the spectra A and B (Fig. 1). This shift is due to the strong hyperfine couplings from the additional methyl group at the N5 position. The best simulation, including three β-protons from the N5-methyl group instead of the N5 α-proton (see Table 1), is depicted in Fig. 1d.

Microwave power saturation behavior of the different pterin radicals

The $P_{1/2}$ value of the microwave power saturation was determined for the radicals shown in Fig. 1. The radical with full-length BH_4-containing nNOS yielded $P_{1/2}$=10±2.5 μW at 4 K, whereas that obtained with eNOS oxygenase domain was characterized by the values of 38±5 μW at 4 K, 1.9±0.2 mW at 9 K, and 21±4 mW at 30 K. For the 6-methyl-PH_4 derived radical we obtained a value of 0.89±0.1 mW at 9 K.

Discussion

Formation of a pterin-derived radical in the reaction of NOS with Arg

On the basis of low-temperature optical spectroscopic studies we previously postulated that a trihydropterin radical is transiently formed when reduced nNOS reacts with O_2 in the presence of Arg [28]. The present results fully confirm this hypothesis. The identification of the observed radicals as pterin centered is based on the following observations: the absolute dependence of the signal on the presence of BH_4, the close similarity of the signal to that of a protonated trihydropterin radical [38], and the changes in signal shape when the experiment is performed with 5-methyl-BH_4 or 6-methyl-PH_4.

The microwave power saturation of the radicals, with a $P_{1/2}$ value of about 1 mW at 9 K, are indicative of magnetic dipolar interaction with another paramagnetic center, which suggests that the radicals were close to the heme iron. This agrees with the three-di-

mensional structures of the catalytic heme domains of iNOS and eNOS that show that BH_4 forms hydrogen bonds to the heme propionate group [5, 6]. From this observation, and from the fact that the radical signal was obtained with full-length BH_4-containing nNOS in the absence of exogenous BH_4, we deduce that all pterin radicals were NOS bound. The BH_4 also takes part in a hydrogen bonding network and aromatic stacking interactions which might be important for electron transfer reactions between cofactors in the full-length protein [39, 40, 41].

Recently, Marletta and co-workers [29] reported the formation of a similar pterin radical with the iNOS oxygenase domain. Using an enzyme preparation containing endogenous BH_4, we were able to demonstrate pterin radical formation from the cofactor bound as a prosthetic group to the active site of NOS. In the Marletta study [29], exogenous BH_4 was added to the pterin-free oxygenase domain of iNOS. Our observations, with both constitutive enzymes and with full-length NOS, demonstrate that pterin radical formation is not peculiar to the oxygenase domain, and is common to all isoforms. In this study we applied sodium dithionite rather than NADPH with full-length NOS for two reasons. Using sodium dithionite allowed direct comparison with our previous low-temperature optical studies. Moreover, since reduction by dithionite is achieved without Ca^{2+}/calmodulin, ambiguities in the assignments of the radical signals to BH_4 instead of the flavins are avoided. Marletta and co-workers [29] reported a maximal radical yield of 80%. The lower yields we obtained (23%) are due to the fact that the optimal radical concentrations were reached and decay had set in before the EPR samples were frozen. Furthermore, ethylene glycol greatly decreases the pterin affinity of NOS[1]. This explains the apparent difference between the yields obtained with full-length BH_4-containing nNOS and with eNOS in the presence of BH_4. The absence of radical signals with NOHLA instead of Arg agrees with prior observations [29], and can be explained by the different electron requirements of the two reaction cycles. Formation of NOHLA from Arg consumes in total two electrons, resulting in heme oxidation and transient formation of a pterin radical. The first electron stems from the flavins (under our conditions from dithionite), and we show that the second electron stems from BH_4, which has to be re-reduced in order to be available for the next reaction cycle. During normal catalysis this pterin radical re-reduction electron may be furnished by the reductase domain, but under the single-turnover and cryo conditions of this study this electron must come from elsewhere (see below). The slowness of this unphysiological reaction together with the low temperature allow detection of the radical intermediate. Formation of citrulline from NOHLA consumes just one electron. Therefore, even if electron transfer from BH_4 to the superoxide complex is an obligatory step in the reaction cycle with NOHLA, the electron will not be consumed during product formation. Consequently, it will be available to rapidly regenerate BH_4, and accumulation of the radical on the timescale of our experiments is not to be expected. Indeed, we observed complete oxidation of the ferrous enzyme within the mixing time of the experiment with optical spectroscopy at –30 °C [42]. Consequently, the present study does not allow us to determine whether a pterin radical is transiently formed in the second cycle. The small amplitude of the radical signal in the absence of substrate confirms that appreciable reductive oxygen activation requires both BH_4 and Arg [43, 44, 45].

Assignment of pterin radicals as protonated trihydrobiopterin radical cations

The experimental spectra were simulated in order to assign changes in signal shape to the different molecular structures of the pterin analogs. Different N5-protonated or -methylated trihydropterin radicals have been investigated earlier at room temperature in solution, where the linewidth is small and the contributions of hfc from different nuclei can readily be detected [32, 33, 34, 35]. Isotropic hfc tensors were determined in the range of 10 G for nitrogen (I=1) and α- and β-protons (I=1/2). It was shown that the spin is mainly confined to N5 and a smaller amount is distributed to N8 [35]. This is readily explained by the four resonance structures (Scheme 1) possible without introducing charge separations, allowing only spin density on N5, N8, C8a, and C2.

Considerable spin density on C8a and/or C2 implies hfc with more than the two nitrogen atoms observed (N5 and N8), which was not found [33, 35]. Thus, the latter two resonance structures are negligible, as indicated by the parentheses.

In powder spectra of frozen samples, anisotropic contributions are governing the shape of the EPR spectra. To demonstrate the effects of hyperfine interaction with the nitrogen nucleus and different kinds of hydrogen nuclei on the radical signal shape, powder simulations of a simplified model with spin density only on N5 are shown in Fig. 2. Figure 2A shows the simulated spectrum of hfc to one nitrogen. The two

[1] The EC_{50} value for BH_4 stimulating L-citrulline formation by full-length nNOS increased from 40 nM in aqueous buffer to 20 μM in the presence of 50% ethylene glycol [42]. The reason for the effect was not investigated; it may be a general solvent effect on the activity of BH_4 or on the structure of the pterin binding site. Alternatively, it may be due to direct competition between BH_4 and ethylene glycol. Inspection of crystal structures of eNOS oxygenase domain obtained in the presence of 30% glycerol [41] (PDB structures 1NSE, 2NSE, 3NSE, 4NSE) shows glycerol molecules occupying the pterin binding sites in the absence of BH_4. Moreover, a further molecule of glycerol is bound in close proximity to the pterin binding site (shortest distance to BH_4, 2.6 Å). It is conceivable that ethylene glycol behaves similarly and in this way affects pterin binding

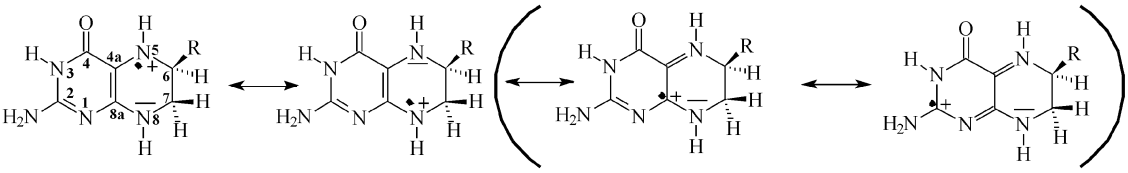

Scheme 1

smaller outer peaks in Fig. 2A explain readily the broad wings of the neighboring β-proton (H_β) on C6 in Fig. 2B. Inclusion of such a proton corresponds to a neutral BH_3• radical but was not sufficient for simulating (Fig. 2B) our signal (Fig. 2D). Thus, N5 must be protonated and an hfc tensor for an α-proton was added. Fitting these three tensors (for N5, N5-H_α, and C6-H_β, corresponding to a protonated BH_3•H^+ radical cation) to the experimental spectrum in Fig. 2D yields a fair simulation (Fig. 2C), but with a much too anisotropic β-proton tensor (see legend of Fig. 2). Thus, the latter is obviously a mixture of the real C6-β-proton tensor and weaker, anisotropic contributions due to a considerable spin density on N8, and therefore interaction with its α-proton N8-H_α, and the two β-protons C7-$H_{\beta1,2}$.

Taken together, we assign the EPR signals to BH_3•H^+ radicals, i.e. $N5^+$-H- or $N5^+$-CH_3-6,7,8-trihydro(bio) pterin radical cations. Marletta and coworkers [29] also assigned the radical EPR signal they observed to a trihydrobiopterin radical, but did not determine its protonation state. When we used the hfc tensors we derived for BH_3•H^+ formed in the oxygenase domain (Table 1) and assumed D_2O exchangable protons on N5 and N8, we were able to simulate the spectral changes caused by D_2O that were reported by Marletta and co-workers [29]. This suggests that the radical obtained with the iNOS oxygenase domain is protonated as well (data not shown).

An advanced model including all seven (nine for 5-methyl-BH_4) hfc was constructed and the tensor-sets, obeying all theoretical and geometrical restrictions to a reasonable degree, achieved for the best least-square fits are listed in Table 1. The corresponding simulations are displayed together with the observed spectra in Fig. 1a, b, c, and d. The isotropic hfc constants, and thus the spin densities on the nitrogens N5 and N8, are in good agreement with those found earlier at room temperature [32, 33, 34, 35], as well as with the recent molybdopterin radical [46] (9 G for N5 and 15 G for C6-H_β). Most satisfying, however, are the dihedral angles θ, not only that the two β-protons on C7 are separated by the expected 120° but also the combination of about 40° on C6 and 10°/130° on C7 is in perfect agreement with the crystal structure of the pyrazine ring [47]. Taken together, in spite of the low resolution of our EPR signals (typical for radicals in frozen solutions), the hfc tensors used for the simulation are likely to give a correct interpretation as they fulfill not only the physical but also the geometrical requirements. On the other hand, this means that the set of hfc tensors found (Table 1) is unique if one assumes a pterin-based radical with similar electronic and geometrical structure as has been determined by room-temperature EPR [32, 33, 34, 35] and X-ray crystal structure [47], respectively. To appreciate the uniqueness of the simulations it is important to note that the fitting parameters are not independent. The main variants are actually the spin densities ρ on N5 and N8 and the dihedral angles θ of the respective β-protons, as they determine the isotropic hfc constants.

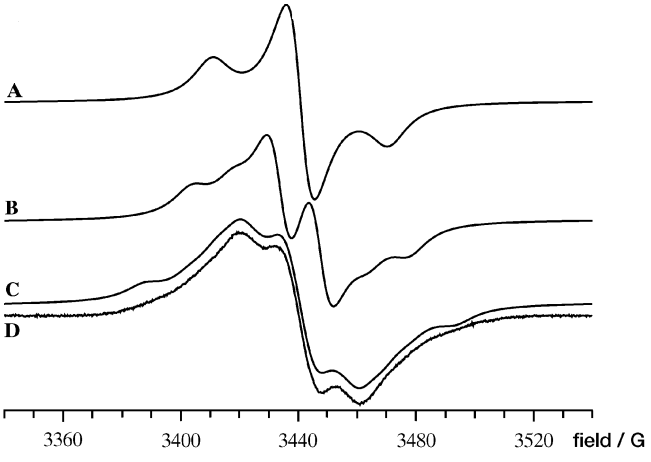

Fig. 2 Effects of the three strongest nuclear couplings on the shape of the EPR signal. *A* Simulation of the anisotropic coupling of a lone electron in a p-orbital of ^{14}N (3, 3, 30) (all values in G) as is expected for N5 in a pterin radical. *B* Simulation including *A*+a β-proton (13, 13, 14), values expected for the proton on C6. This spectrum is roughly expected for a neutral BH_3• radical. *C* Fit of *B* plus an α-proton tensor. *D* Experimentally obtained spectrum, identical to Fig. 1A, shown here for comparison. The simulation represents the experimental spectrum quite well and yields a typical nitrogen hfc tensor (3.8, 3.8, 33.5), a reasonable α-proton tensor (–1.6, –15.5, –20.7) (the minus sign is assumed from theory), but a β-proton tensor (5.9, 4.8, 25.1) which is much too anisotropic, indicating considerable spin density on N8

Simulation-derived explanations for EPR signal differences

The different shapes of the spectra in full-length nNOS (Fig. 1A) and in the eNOS oxygenase domain (Fig. 1B) cannot be explained by differences in linewidth. However, the anisotropic part of the N5-H_α tensor in the spectrum of Fig. 1b (+8.3, –9.4, +1.1) shows a symmetry much closer to theory ($T_x \approx -T_y$, $T_z \approx 0$) than in the spectrum of Fig. 1a (+9.0, –5.8, –3.1). In a similar way, the tensor of the C6-H_β in

Fig. 1b shows a much smaller anisotropy (0, –1.5, +1.6) than that in Fig. 1a (–5.5, 0, +5.5). N5 and N8 are assumed to be in one plane with the pyrimidine ring, as found in crystal structures of several pterins [47, 48, 49]. In the crystal structure of the BH_4-containing eNOS oxygenase domain, the N5 side is hydrogen bonded to glycerol [6]. As the position of a solvent molecule is flexible, this should result in a relaxed structure of the pterin. This is reflected by the hfc tensors of the BH_3•H^+ radical formed in the eNOS oxygenase domain (Table 1, Fig. 1B and b), as they completely fulfill theoretical expectations in the error margins of our simulations. The slightly different anisotropic parts in the full-length nNOS (Table 1, Fig. 1A and a) indicate some distortion from the assumed planarity, e.g. rotation of N5 and its α-proton out of the ring plane. Whether this distortion is due to a slight conformational change in the pterin binding site brought about by the presence of the reductase domain in full-length nNOS, or to distinct features of the BH_4 binding sites in full-length eNOS and nNOS, has to await further investigations.

Replacing the L-*erythro* group at C6 by methyl gives a surprisingly different signal shape for 6-methyl-PH_4 in the eNOS oxygenase domain (Fig. 1C). Its simulation (Fig. 1c) yields a significant increase of spin density on N8 from about 0.08 to 0.11 and thus larger hfc tensors for both C7-H_β without affecting the spin density on N5 (Table 1). The expected broadening for the 5-methyl-BH_4-derived spectrum is only insufficiently simulated by the three β-protons of the N5-methyl group replacing the N5-H_α, but a further increase of spin density on N8 to ρ=0.14 is required for a good simulation (Fig. 1d, Table 1). For both cases we propose that structural and/or electronic changes in the pyrazine ring draw spin density out of the pyrimidine ring, where it is delocalized, towards N8.

Mechanism of re-reduction of the pterin radical

How is the BH_3•H^+ radical reduced back to BH_4? Reduction from the flavins in the reductase domain is excluded in our experiments at –30 °C, as we used either the eNOS oxygenase domain or full-length nNOS without calmodulin. Electron transfer from dithionite is excluded at –30 °C as well [28]. We propose therefore that under our special conditions the BH_3•H^+ radical is reduced back to BH_4 by the ferrous heme of the second subunit. The sole additional EPR signal detected in these experiments was a high-spin (S=5/2) Fe(III) signal at g-values of 7.7, 4.1, and 1.8 (data not shown), most likely originating from re-oxidized heme. These signals may derive partly from the heme in the subunit after complete oxidation, and partly from the heme in the second subunit after electron transfer to BH_3•H^+, in line with the low radical yields observed by us.

Interestingly, we did not detect any known compound I-associated radical signals under these NOS experiments, such as the porphyrin π^+, tryptophyl, or tyrosyl radicals that have been reported for cyt P450 and horseradish peroxidase [50, 51, 52], for cytochrome *c* peroxidase [53, 54], and for prostaglandin H_2 synthetase [55, 56], respectively. Our studies clearly demonstrated that BH_4 is required for reductive activation of the superoxide complex under formation of a pterin radical. With the existence of such radicals firmly established, one may now speculate that an additional function of BH_4 consists in the stabilization of compound I. In this respect the BH_3•H^+ radical might perform the same function that has previously been reported for the porphyrin π^+ radical. The location of BH_4 in close vicinity to the heme makes it a likely candidate for such a role. At this point we can neither confirm nor refute this possibility [6, 57, 58].

Conclusion

This is the first report of a protonated trihydropterin radical cation intermediate in the catalytic cycles of nNOS and eNOS and in any monooxygenase. Moreover, we observed pterin radicals with the full-length enzyme, and in the presence of endogenous BH_4 only. We were able to show radical formation by pterin derivatives other than BH_4, yielding important information on the structure of the radical. The combined use of substituted pterins and simulation of the obtained EPR spectra indicates formation of cationic BH_3•H^+ radicals rather than BH_3• radicals by both full-length nNOS and the oxygenase domain of eNOS. This important mechanistic information was lacking in the earlier investigation by Marletta and co-workers [29]. These observations offer strong support for our proposal that the main function of BH_4 in NOS catalysis is as a one-electron donor during reductive oxygen activation [28], a concept which conflicts with the consensus that regards BH_4 mainly as an allosteric effector. This study has also relevance for the aromatic amino acid hydroxylases since pterin radicals have been suggested to be involved at various stages of their catalytic cycle [57, 59].

Acknowledgements This work was financed by the Norwegian Research Council (K.K.A.), the Norwegian Cancer Society (K.K.A.), the TMR and Biotechnology programmes of the EU (ERBMRFXCT980207 and BIO4-98-0385) (K.K.A.), and the Fonds zur Förderung der Wissenschaftlichen Forschung in Austria, grants 13586-MED (B.M.), 13013-MED (B.M.), and 13793-MOB (E.R.W.). We thank Prof. E. Sagstuen for valuable discussions about the theory of hfc tensors.

References

1. Griffith OW, Stuehr DJ (1995) Annu Rev Physiol 57:707–736
2. Mayer B, Hemmens B (1997) Trends Biochem Sci 22:477–481
3. Gorren ACF, Mayer B (1998) Biochemistry (Moscow) 63:870–880
4. Stuehr DJ (1999) Biochim Biophys Acta 1411:217–230
5. Crane BR, Arvai AS, Gachhui R, Wu C, Ghosh DK, Getzoff ED, Stuehr DJ, Tainer JA (1997) Science 278:425–431
6. Raman CS, Li H, Martásek P, Král V, Masters BSS, Poulos TL (1998) Cell 95:939–950
7. Marletta MA, Hurshman AR, Rusche KM (1998) Curr Opin Chem Biol 2:656–663
8. Poulos TL, Raman CS, Li H (1998) Structure 6:255–258
9. Holm RH, Kennepohl P, Solomon EI (1996) Chem Rev 96:2239–2314
10. White RE, Coon MJ (1980) Annu Rev Biochem 49:315–356
11. Ortiz de Montellano PR (1986) In: Ortiz de Montellano (ed) Cytochrome P-450: structure, mechanism, and biochemistry. Plenum Press, New York, pp 217–271
12. Guengerich FP (1990) Crit Rev Biochem Mol Biol 25:97–153
13. Mueller EJ, Loida PJ, Sligar SG (1995) In: Ortiz de Montellano (ed) Cytochrome P450: structure, mechanism, and biochemistry, 2nd edn. Plenum Press, New York, pp 83–124
14. Andersson KK, Debey P, Balny C (1979) FEBS Lett 102:117–120
15. Poulos TL (1997) Curr Opin Struct Biol 5:767–774
16. Sundaramoorthy M, Terner J, Poulos TL (1998) Chem Biol 5:461–473
17. Mayer B,Werner ER (1995) Naunyn-Schmiedeberg's Arch Pharmacol 351:453–463
18. Perry JM, Marletta MA (1998) Proc Natl Acad Sci USA 95:11101–11106
19. Kappock TJ, Caradonna JP (1996) Chem Rev 96:2659–2756
20. Riethmüller C, Gorren ACF, Pitters E, Hemmens B, Habisch H-J, Heales SJR, Schmidt K, Werner ER, Mayer B (1999) J Biol Chem 274:16047–16051
21. Baek KJ, Thiel BA, Lucas S, Stuehr DJ (1993) J Biol Chem 268:21120–21129
22. Klatt P, Schmidt K, Lehner D, Glatter O, Bächinger HP, Mayer B (1995) EMBO J 14:3687–3695
23. McMillan K, Masters BSS (1995) Biochemistry 34:3686–3693
24. Ghosh DK, Abu-Soud HM, Stuehr DJ (1996) Biochemistry 35:1444–1449
25. Klatt P, Schmid M, Leopold E, Schmidt K, Werner ER, Mayer B (1994) J Biol Chem 269:13861–13866
26. Gorren ACF, List BM, Schrammel A, Pitters E, Hemmens B, Werner ER, Schmidt K, Mayer, B (1996) Biochemistry 35:16735–16745
27. Pfeiffer S, Gorren ACF, Pitters E, Schmidt K, Werner ER, Mayer B (1997) Biochem J 328:349–352
28. Bec N, Gorren ACF, Völker C, Mayer B, Lange R (1998) J Biol Chem 273:13502–13508
29. Hurshman AR, Krebs C, Edmondson DE, Huynh BH, Marletta MA (1999) Biochemistry 38:15689–15696
30. Harteneck C, Klatt P, Schmidt K, Mayer B (1994) Biochem J 304:683–686
31. Eloranta J (2000) ftp://epr.chem.jyu.fi/pub/xemr
32. Ehrenberg A, Hemmerich P, Müller F, Okada T, Viscontini M (1967) Helv Chim Acta 50:411–416
33. Bobst A (1968) Helv Chim Acta 51:607–613
34. Ehrenberg A, Hemmerich P, Müller F, Pfleiderer W (1970) Eur J Biochem 16:584–591
35. Westerling J, Mager HIX, Berends W (1977) Tetrahedron 33:2587–2594
36. Carrington A, McLachlan AD (1969) Introduction to magnetic resonance. Harper & Row, New York, p 94
37. Himo F, Gräslund A, Eriksson LA (1997) Biophys J 72:1556–1567
38. Bobst A (1967) Helv Chim Acta 50:2222–2225
39. Ghosh S, Wolan D, Adak S, Crane BR, Kwon NS, Tainer JA, Getzoff ED, Stuehr DJ (1999) J Biol Chem 274:24100–24112
40. Sagami I, Sato Y, Daff S, Shimizu T (2000) J Biol Chem 275:26150–26157
41. Li H, Raman CS, Glaser CB, Blasko E, Young TA, Parkinson JF, Whitlow M, Poulos TL (1999) J Biol Chem 274:21276–21284
42. Gorren AC F, Bec N, Schrammel A, Werner ER, Lange R, Mayer B (2000) Biochemistry 39:11763–11770
43. Mayer B, John M, Heinzel B, Werner ER, Wachter H, Schultz G, Böhme E (1991) FEBS Lett 288:187–191
44. Heinzel B, John M, Klatt P, Böhme E, Mayer B (1992) Biochem J 281:627–630
45. Pou S, Pou WS, Bredt DS, Snyder SH, Rosen GM (1992) J Biol Chem 267:24173–24176
46. Luykx DMAM, Duine JA, de Vries S (1998) Biochemistry 37:11366–11375
47. Bieri JH, Viscontini M (1977) Helv Chim Acta 60:1926–1931
48. Bieri JH, Viscontini M (1977) Helv Chim Acta 60:447–453
49. Bieri JH (1977) Helv Chim Acta 60:2303–2308
50. Larroque C, Lange R, Maurin L, Bienvenüe A, van Lier JE (1990) Arch Biochem Biophys 282:198–201
51. Blumberg, WE, Peisach J, Wittenberg BA, Wittenberg JB (1968) J Biol Chem 243:1854–1862
52. Palcic MM, Rutter R, Araiso T, Hager LP, Dunford B (1980) Biochem Biophys Res Commun 94:1123–1127
53. Goodin DB, Mauk AG, Smith M (1987) J Biol Chem 262:7719–7724
54. Goodin DB, Mauk AG, Smith M (1986) Proc Natl Acad Sci USA 83:1295–1299
55. Karthein R, Dietz R, Nastainczyk W, Ruf HH (1988) Eur J Biochem 171:313–320
56. Prince RC (1988) Trends Biochem Sci 13:286–288
57. Andersson KK, Gräslund A (1995) Adv Inorg Chem 43:359–408
58. Crane BR, Arvai AS, Ghosh S, Getzoff ED, Stuehr D J, Tainer JA (2000) Biochemistry 39:4608–4621
59. Fitzpatrick PF (1999) Annu Rev Biochem 68:355–381